Heavy flavor production at RHIC and LHC energy

A. K. Chaudhuri*
Variable Energy Cyclotron Centre
1/AF,Bidhan Nagar, Kolkata - 700 064

In a leading order pQCD model, we have studied the heavy flavor production in p+p collisions at RHIC and LHC energy. Leading order pQCD models require a K-factor. At RHIC energy, $\sqrt{s}$=200 GeV, we fix K such that the model reproduces the integrated charm yield, $dN^{c\bar{c}}/dy$, estimated by the STAR and the PHENIX collaboration in p+p collisions. The model then explains the STAR data on the transverse momentum distribution of open charm mesons (D^0) and decay electrons in p+p collisions. The p+p predictions, scaled by the number of binary collisions, also explain the electron spectra in STAR p+d collisions and PHENIX Au+Au collisions in different centrality bins. Assuming that at LHC energy K-factor is of the order of unity, we have used the model to predict the transverse momentum distribution of D and B mesons and also of electrons from semileptonic decay of $D \to e$ and $B \to e$, in p+p collisions at LHC energy, $\sqrt{s}$=14 TeV.

I. INTRODUCTION

Recently STAR collaboration has measured the transverse momentum distribution of open charm mesons, $D^0(\bar{D}^0)$ from direct reconstruction of $D^0(\bar{D}^0) \to K^{\mp}\pi^{\pm}$ in d+Au collisions and indirect electron-position measurements via charm semileptonic decays in p+p and d+Au collisions at $\sqrt{s}$=200 GeV [1]. Electron spectra show approximate binary collision scaling between p+p and d+Au collisions. The total charm cross section per nucleon-nucleon interaction for d+Au collisions at $\sqrt{s}$=200 GeV is $\sigma^{c\bar{c}} = 1.3 \pm 0.2 \pm 0.4$ mb, considerably larger than the standard PYTHIA prediction. Semileptonic decay spectra of electrons has also been measured by the PHENIX collaboration [2] in p+p and in Au+Au collisions, at $\sqrt{s}$=200 GeV. In Au+Au collisions, PHENIX measured charm electrons in different centrality bins. PHENIX data also indicate that the binary collision scaling holds for charm production in Au+Au collisions. However, PHENIX measured lesser number of charm. Their estimate, $\sigma^{c\bar{c}} = 622 \pm 57 \pm 160$ μb, is approximately one half of the STAR estimate. PHENIX Au+Au charm results are in contrast with the strong violation of binary collision scaling observed in non-charmed (light) hadrons. All the four RHIC experiments, STAR, PHENIX, PHOBOS and BRAHMS reported large suppression of high p_T (light) hadrons in Au+Au collisions [3–6]. High p_T suppression of non-charmed (Light) hadrons are generally explained in terms of partonic energy loss in a dense medium [7,8]. Indeed, they are the most important inputs for the claim that very high density medium is created at RHIC Au+Au collisions. However the charm results are not contradictory with the high p_T suppression observed in non-charmed hadrons. Energy loss do not reduce the number of partons, rather change the p_T distribution. Thus if in Au+Au collisions, heavy quarks suffered energy loss, momentum distribution of charmed electrons would not have scaled with charmed electron distribution in pp collisions. The PHENIX Au+Au data on charm electrons then confirm the believe that heavy quarks suffer no or little energy loss in the medium.

Theoretical understanding of heavy flavor production is of considerable interest. Perturbative QCD is better applicable for heavy flavor production. Their large mass provide a natural scale for perturbative expansion. Experimental data on heavy flavor production can test the perturbative models and provide important inputs like various mixing angles. In heavy ion collisions at RHIC, heavy flavor production can give important information about the initial condition of the medium produced. Due to their large mass, heavy flavors are produced in initial hard collisions and in a short time scale and are ideal probe for the initial condition of the medium produced. Passage of a heavy flavor through a deconfined medium can alter the momentum distribution of heavy flavored hadrons. Semileptonic decay of a heavy flavored hadron $D(B) \to Xe\nu$, add to the charmonium background, an important signal of the confinement-deconfinement phase transition. Open charm yield is also important for understanding charmonium production. Quite early, Matsui and Satz [9] suggested that charmoniums will be suppressed in a deconfined medium. However, recently there have been suggestions that rather than suppression, at RHIC, charmonium yield will be enhanced due to recombination effect [10]. Open charm yield can help to decipher the issue of suppression/enhancement of charmoniums.

Heavy flavor production in pQCD models has been studied earlier also [11–13]. Recently Cacciari et al [13] made an up-to-date prediction for open charm and bottom production at RHIC p+p collisions, using the First Order plus Next-to-leading-Log (FONLL) level. In the present paper, we have studied heavy flavor production in a leading order

pQCD model. Leading order pQCD models are simpler but need a K-factor. K factor accounts for the neglect of all the higher order terms in the perturbative expansion. K-factor depends on energy. Energy dependence of K-factor has been studied in [14]. K-factor decreases with energy and at RHIC energy, $K \sim 3.4$. At still higher energy K factor approaches unity. In the present paper, at RHIC energy K is obtained by fitting the integrated charm yield $dN^{c\bar{c}}/dy$ in STAR and PHENIX p+p collisions. With the K-factor so fixed, the model is used to explain the STAR and PHENIX data on the transverse momentum distribution of D-mesons and decay electrons. As it will be shown later, the model, with heavy quark fragmentation function, parameterised by Braaten et al [15], give excellent description to STAR and PHENIX data. The more well known Peterson's fragmentation function [16] underpredict the data by a factor of 3 or so. The model can serve as a baseline for comparing heavy flavor data in RHIC Au+Au collisions and in future LHC energy collisions.

The paper is organised as follows: in section 2, we briefly describe the pQCD model. Results for heavy flavor production and comparison with RHIC experiments (STAR and PHENIX) are done in section 3. Model predictions for heavy meson production and decay electrons at LHC energy, $\sqrt{s}$=14 TeV p+p collisions are also given in sec.3. Summary and conclusions are given in section 4.

II. PCQD MODEL OF CHARM QUARK AND CHARMED MESON PRODUCTION

In pQCD models, semileptonic decay of a heavy meson, occur in three step: (i) production of a heavy quark in parton level collisions, (ii) fragmentation of the heavy quark in to a heavy mesons and (iii) semileptonic decay of heavy meson. Schematically transverse momentum spectra of decay electrons in p+p collisions can be written as (schematically),

$$\frac{d\sigma^e}{dydp_T^2} = \frac{d\sigma^Q}{dy_Q d^2p_{T_Q}} \bigotimes D(Q \to H_Q) \bigotimes f(H_Q \to e) \tag{1}$$

where the symbol $\bigotimes$ denote generic convolution and $D(Q \to H_Q)$ and $f(H_Q \to e)$ represent the fragmentation of heavy quark Q into a heavy flavored hadron H_Q, and semileptonic decay of H_Q into electron respectively.

Detail of the evaluation of Eq.1 is given in the appendix. For evaluation of Eq.1, parton distribution functions and fragmentation function of a heavy quark to fragment into a heavy hadron, are required. For the parton distributions, we have used CTEQ5L parameterisation. Several fragmentation function have been used in literature [15–18]. Most well known is the parameterisation by Peterson et al [16]. Peterson's parameterisation does not contain spin information and is parameterised as,

$$D_{c/C}(z) = \frac{N}{z[1 - 1/z - \varepsilon_Q/(1-z)]^2} \tag{2}$$

here N is the normalisation and ε_Q is a parameter. The parameter ε_Q is approximately the ratio of square of constituent light quark (q) and heavy quark (Q) masses, $\varepsilon_Q = m_q^2/m_Q^2$. $\varepsilon_Q = m_q^2/m_Q^2$ depend on the heavy quark mass. Most commonly used values are, $\varepsilon_Q = 0.5$ for fragmentation of a charm quark into a D-meson and $\varepsilon_Q = 0.006$ for fragmentation of a bottom quark into a B-meson. More recently Braaten et al [15] parameterized the heavy quark fragmentation function. It contains the spin information. The pseudo-scalar and vector meson fragmentation functions are written as,

$$\begin{aligned} D_{Q\to P}(z) = N\frac{rz(1-z)^2}{[1-(1-r)z]^6}[6 - 18(1-2r)z + (21 - 74r + 68r^2)z^2 - 2(1-r)(6 - 19r + 18r^2)z^3 + \\ 3(1-r)^2(1-2r+2r^2)z^4] \end{aligned} \tag{3}$$

$$\begin{aligned} D_{Q\to V}(z) = N\frac{rz(1-z)^2}{[1-(1-r)z]^6}[2 - 2(3-2r)z + 3(3-2r+4r^2)z^2 - 2(1-r)(4-r+2r^2)z^3 + \\ (1-r)^2(3-2r+2r^2)z^4] \end{aligned} \tag{4}$$

Parameter r is approximately the ratio of constituent quarks masses, $r = m_q/m_Q$. $r = 0.1$ for c-quark fragmentation to D-mesons, and $r = 0.03$ for fragmentation of b-quarks into a B-meson. In the present work we have used the pQCD pseudo-scalar fragmentation functions parameterised by Braaten et al [15], henceforth call FF-I. For comparison, we will present results obtained with the fragmentation function parameterised by Peterson et al [16] (henceforth call FF-II). As will be shown later, fragmentation function FF-II yields are nearly a factor of two less than the yield obtained from FF-I. Peterson's fragmentation function is comparatively hard.

Fragmentation functions, Eq.2 and 3 are used as the initial distribution at momentum scale, $q^2 = m^2_{c(b)}$. In the present work, we have used m_c=1.5 GeV and m_b=4.4 GeV as charm and bottom quark mass respectively. Fragmentation function at other momentum scales are obtained from numerically integrating the Alterelli- Parisi evolution equation,

$$\mu^2 \frac{\partial}{\partial \mu^2} D_{Q_H}(z,\mu^2) = \int_z^1 \frac{dy}{y} P_{Q\to Q}(\frac{z}{y},\mu) D_{Q\to H}(y,\mu^2) \tag{5}$$

where $P_{Q\to Q}$ is the splitting function:

$$P_{Q\to Q}(z,\mu^2) = \frac{2\alpha_s(\mu^2)}{3\pi}\left(\frac{1+z^2}{1-z}\right)_+ \tag{6}$$

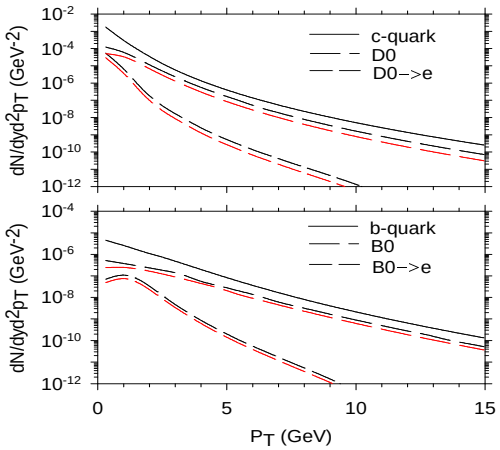

FIG. 1. (a) Solid line is the pQCD prediction for the p_T distribution of c-quarks at $\sqrt{s}$=200 GeV with K=1. The dashed and short-dashed lines are the model predictions for D^0-mesons and decay electrons with FF-I. Red dashed line and short dashed lines are the model predictions for D-meson and decay electrons with FF-II. (b) same for b-quarks, B-mesons and $B \to e$ decay.

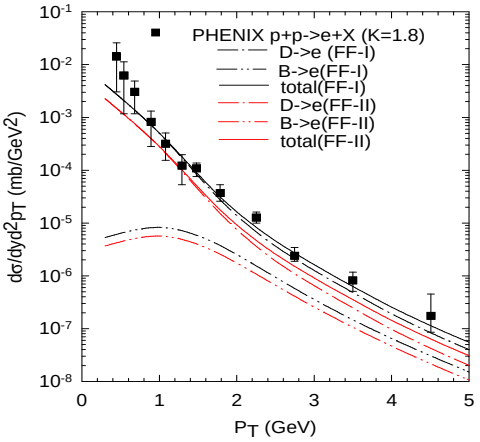

FIG. 2. PHENIX measurements of p_T distribution of charm electrons in p+p collisions at RHIC energy, $\sqrt{s}$=200 GeV. The pQCD predictions with FF-I , are shown as dash-dot and dash-dot-dot lines, for D and B meson decay respectively. The solid line is the sum of the two contributions. Results obtained with FF-II are shown as red lines. The K-factor is 1.8.

III. RESULTS

A. Transverse momentum distribution of D^0,B^0 and semileptonic decay electrons at RHIC

The pQCD model predictions for the transverse momentum distribution of heavy mesons and decay electrons in $\sqrt{s}$=200 GeV p+p collisions are shown in Fig.1a and 1b. Here we have taken K=1. In Fig.1a, solid black line is the p_T spectrum for charm quarks. Charm quark fragmentation to D mesons and semileptonic decay of D-mesons, obtained with the fragmentation function FF-I is shown as black dashed and short-dashed lines respectively. The same obtained with the fragmentation function FF-II are shown as red dashed and red short-dashed lines. p_T distribution of D-mesons closely scale with c-quarks but p_T distribution of electrons falls much faster than that of c-quarks or of D-mesons. We also note that yield of D mesons and also of decay electrons, obtained with the fragmentation function FF-I are approximately a factor of 2 larger than the yield obtained with the parameterisation FF-II. Peterson fragmentation function (FF-II) is comparatively hard. Same results, for bottom production are shown in Fig.1b. At RHIC energy, low p_T heavy quarks are dominantly charm. Heavy mass of bottom quarks inhibit their production at low p_T. However, at large p_T, bottom production evenly competes with charm production. Consequently, at large p_T semileptonic decay electrons will have contributions from D as well as from B mesons. For B-mesons also fragmentation function FF-II produces factor of two less number of B-mesons than the fragmentation function FF-I.

As mentioned earlier, leading order pQCD models require a k-factor. STAR and PHENIX collaboration had estimated the total charm yield in p+p collisions at $\sqrt{s}$=200 GeV. While the PHENIX collaboration [2] obtained $d\sigma^{c\bar{c}}/dy = 143 \pm 13 \pm 36$ μb in the p_T range, $0.4GeV < p_T < 4GeV$, the STAR collaboration [1] obtained larger value, $d\sigma^{c\bar{c}}/dy = 0.29 \pm 0.04 \pm 0.08$ mb in p_T range, $1GeV < p_T < 4GeV$. We have fixed the K factor such that the integrated charm yield in the model reproduces the central value of the PHENIX and STAR estimate. We obtain, K=1.8 and K=7.0 for PHENIX and STAR experiment respectively. We could have fixed K to reproduce the D meson or the electron yield. But fixing the K from charm yield has the advantage that the model can now test different fragmentation functions by comparing the model predictions with experiment. Before we continue we note that the large uncertainty in K (K=1.8 for PHENIX experimental data and 7.0 for STAR experimental data)is a direct result of large difference in integrated charm cross sections in two measurements. We hope that in future the large difference in charm cross sections, in two experiments, will be removed. and K can be fixed more accurately.

With the only parameter of the model fixed, we can compare model predictions with other experimental observable, namely, p_T distribution of D^0 and decay electrons in STAR and PHENIX experiments. In Fig.2, p_T distribution of charm electrons in pp collisions, measured by the PHENIX collaboration [4] at $\sqrt{s}$=200 GeV is shown. Present pQCD model predictions obtained with the fragmentation functions FF-I (black lines) and FF-II (red lines) are also shown in Fig.2. For both the fragmentation functions, the K-factor is fixed, K=1.8. We have shown the contribution of both D (the dash-dot line) and B mesons (dash-dot-dot line) decay. Solid lines are the sum of the two contributions. At low p_T, decay of B-mesons contribute negligibly to the total electron spectrum. For p_T <2 GeV, bottom contribute less than 10% to the total yield. In the p_T range 2-3 GeV bottom contribute 10-20% and in p_T range 3-4 GeV bottom contribution rises to 20-30%. This numbers compare favorably with PHYTHIA estimate [19]. Present pQCD model with FF-I well reproduces the PHENIX data. On the other hand fragmentation function FF-II, though reproduce the shape of the spectra, underpredict the PHENIX data by a factor of ∼2. This is understood. As mentioned earlier, Peterson's fragmentation functions are hard and it produces less number of heavy mesons.

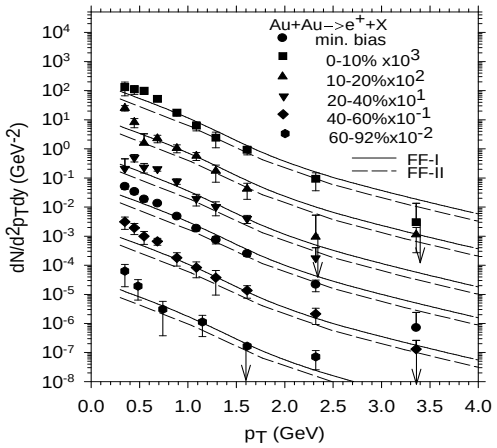

FIG. 3. Transverse momentum distribution of charmed electrons in Au+Au collisions at RHIC energy, $\sqrt{s}$=200 GeV. Solid lines are pQCD predictions (K=1.8) for p+p collisions, scaled by the nuclear overlap function.

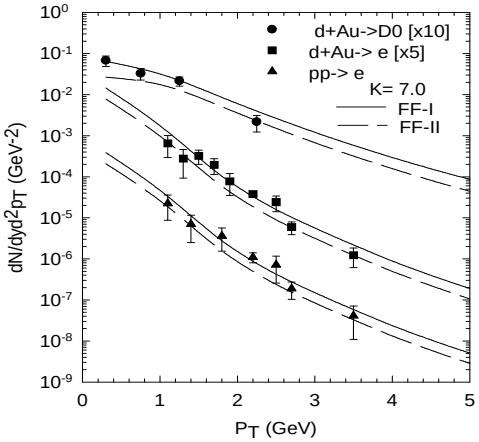

FIG. 4. STAR measurements of p_T distribution D-meson (solid circles) and charmed electrons (solid squares) in d+Au collisions at RHIC energy $\sqrt{s}$=200 GeV. STAR pp results for decay electrons are shown as solid triangle. The solid and dashed lines are the pQCD predictions with FF-I and FF-II respectively with K=7.0 .

In Fig.3, PHENIX measurements [2] in Au+Au collisions, in different centrality bins are shown. As mentioned earlier, charm electrons scale with binary collision numbers. In Fig.3, present pQCD model results, with K=1.8 are shown. The solid and dashed lines are obtained with fragmentation function FF-I and FF-II respectively. We have included the B meson decay contributions. For comparing with PHENIX data the pp-predictions are multiplied by the nuclear overlap function. As expected, model predictions with Braaten parameterisation of fragmentation function agree well with the experiment. Here again, Peterson's parameterisation underpredict the data approximately by a factor of 2. Analysis of PHENIX data confirms that heavy quarks suffer little or no energy loss in the medium produced in Au+Au collisions at RHIC energy.

We now compare the present model predictions with the STAR experiment. STAR collaboration [1] have measured p_T-distribution of D-mesons in d+Au collisions at $\sqrt{s}$=200 GeV. They have also measured the semileptonic decay electrons in d+Au and p+p collisions. In Fig.4, STAR data are shown. As mentioned earlier, for STAR experiment, we use K=7.0 . In Fig.4, solid and dashed lines present model predictions with fragmentation functions FF-I and FF-II respectively. For d+Au collisions, we have multiplied the results for pp predictions by $N_{bin} = 7.5$. We note that the fragmentation function FF-I, with K=7 can describe the STAR data on charm production in p+p, p+d collisions. FF-II, as before leads to poorer description of the data.

B. Transverse momentum distribution of D^0,B^0 and semileptonic decay electrons at LHC

We have shown that the present pQCD model with the heavy quark fragmentation function, parameterised by Braaten et al [15], reproduces the STAR and PHENIX data on the transverse momentum distribution of D meson and semileptonic decay electrons in $\sqrt{s}$=200 GeV p+p, d+Au and Au+Au collisions. With a reasonable estimate of K, the model can be used to predict heavy flavor production in pp collisions at LHC energy, As mentioned earlier, K factor decreases with energy and at LHC energy, expected value is $K \sim 1 - 1.5$ [14]. In the present section, we give predictions for the transverse momentum distribution of D, B and semileptonic decay electrons with K=1. We only show the predictions obtained with the fragmentation function FF-I, parameterised by Braaten et al [15]. As shown earlier, RHIC data are better explained with this parameterisation. Before we proceed, a note of caution is in order. The model is tested against RHIC data, limited to $p_T \leq 4.5$ GeV. Accuracy of the model beyond p_T=4.5 GeV is not tested. In the following, we will show model prediction over a wide range of p_T, but the predictions for $p_T \geq 5$ GeV may not be accurate.

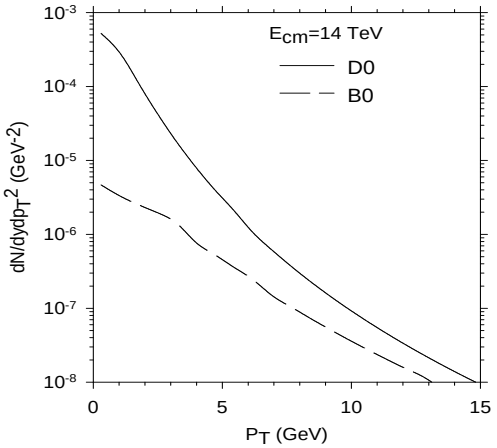

FIG. 5. Transverse momentum distribution of D mesons (solid line) and B mesons (dashed line) in pp collision at LHC energy, $\sqrt{s}$=14 TeV.

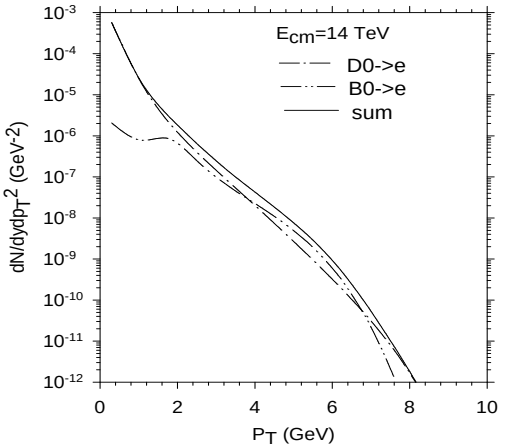

FIG. 6. Transverse momentum distribution of electrons in semileptonic decay of D mesons (dash-dot line), B mesons (dash-dot-dot line) in pp collisions at LHC energy $\sqrt{s}$=14 TeV. The solid line is the sum of the two contributions.

In Fig.5, model predictions, for the transverse momentum distributions of D and B mesons in pp collisions at LHC energy $\sqrt{s}$=14 TeV, are shown. As it was at RHIC energy, at LHC energy also, low p_T heavy mesons are dominated by the D-mesons. At low p_T B-meson yield is significantly lower than the D meson yield. Only at large p_T, B-meson contribute significantly to total heavy meson production. However, compared to RHIC energy (see Fig.1), at LHC energy both D and B meson yields are increased. High p_T yields are significantly increased, by a factor, 1000 or more.

In Fig.6, p_T distribution of electrons from semileptonic decay of D and B meson are shown. Low p_T electron spectra is dominated by the electrons from decay of D-meson. Below p_T=1 GeV, B mesons contribute less than 10% to the total yield. B meson contribution increases rapidly with p_T and in p_T range 2-4 GeV, it rises to 30-50%. However, at very large $p_T > 6GeV$ B mesons contribution decreases again.

IV. SUMMARY AND CONCLUSIONS

In a pQCD based model, we have studied the heavy flavor production at RHIC energy pp collisions. At RHIC energy, heavy flavor production is dominated by the charm quarks. Below p_T=2 GeV, more than 90% heavy quarks are charm. Production of bottom quark picks up only at large p_T and at p_T=5 GeV, it contribute to 20% of to total heavy quark yield. As a consequence of dominance of charm quark at low p_T, at RHIC low p_T heavy mesons are dominantly D-mesons. Similarly decay electrons are dominantly from decay of D meson. We have compared the pQCD model predictions for D and decay electrons with STAR and PHENIX data. This models require a K-factor. At RHIC energy, we fix the K-factor to reproduce the integrated charm yield $d\sigma^{c\bar{c}}/dy$, estimated in STAR and PHENIX experiments. With K-factor fixed from total charm yield, the model, with fragmentation function parameterised by Braaten et al [15], reproduces the transverse momentum spectra of semileptonic decay electrons measured by the PHENIX and STAR collaboration in $\sqrt{s}$=200 GeV p+p collisions. pp predictions scaled by the nuclear overlap function also explain the PHENIX Au+Au charm data in different centrality bins. p_T distribution of D^0 in p+d collisions, measured by the STAR collaboration is also explained in the model. The results confirms that charm production in d+Au and Au+Au collisions obey binary collision scaling law. The other, much used fragmentation function parameterised by Peterson et al [16], though reproduces the shape of the distributions, underpredict the yields by a factor of $\sim$ 2-3. Assuming that at LHC energy, $\sqrt{s}$=14 TeV, K-factor approached unity, we have used the model to predict heavy flavor production in p+p collisions at LHC energy. Compare to RHIC energy, at LHC energy collisions, heavy flavor production is increased. At large p_T increase is more than a factor 1000.

APPENDIX A: PQCD MODEL FOR P_T DISTRIBUTION OF SEMILEPTONIC DECAY OF $D \to XE\nu$

Production cross section of a heavy quark c (charm) in a pp collision can be written as [20]

$$\frac{d\sigma^c}{dyd^2p_T} = K \sum_{i,j}^{partons} \int dx_a dx_b f_i(x_a, Q^2) f_j(x_b, Q^2) \frac{\hat{s}}{\pi} \frac{d\sigma}{d\hat{t}}(ab \to cd) \delta(\hat{s} + \hat{t} + \hat{u} - m_a^2 - m_b^2 - m_c^2 - m_d^2) \tag{A1}$$

where x_a and x_b are the fractional momenta of the colliding partons. $(\hat{s}, \hat{t}, \hat{u})$ are the Mandelstam variables for the subprocess $ab \to cd$. $\frac{d\sigma}{d\hat{t}}$ is the subprocess cross-section. The factor K takes into account the neglect of higher order terms.

For a open charm production subprocesses $ab \to cd$ of interest are:

$$gg \to C\bar{C} \tag{A2}$$
$$q\bar{q} \to C\bar{C} \tag{A3}$$
$$gQ \to gC \tag{A4}$$
$$qQ \to qC \tag{A5}$$

where C denote a charm quark. g and q denote a gluon and a light quark respectively.

Matrix elements for these processes are calculated in [21]. For charm quark mass M subprocess cross sections are,

$$|M|^2_{q\bar{q}\to c\bar{c}} = \frac{64}{9}\pi^2\alpha^2(Q^2)\frac{(M^2-\hat{t})^2 + (M^2-\hat{u})^2 + 2M^2\hat{s}}{\hat{s}^2} \tag{A6a}$$

$$\begin{aligned} |M|^2_{gg\to c\bar{c}} = \pi^2\alpha^2(Q^2)[&\frac{12}{\hat{s}^2}(M^2-\hat{t})(M^2-\hat{u}) + \frac{8}{3}\frac{(M^2-\hat{t})(M^2-\hat{u}) - 2M^2(M^2+\hat{t})}{(M^2-\hat{t})^2} \\ &+\frac{8}{3}\frac{(M^2-\hat{t})(M^2-\hat{u}) - 2M^2(M^2+\hat{u})}{(M^2-\hat{u})^2} - \frac{2}{3}\frac{M^2(\hat{s}-4M^2)}{(M^2-\hat{t})(M^2-\hat{u})} \\ &-6\frac{(M^2-\hat{t})(M^2-\hat{u}) + M^2(\hat{u}-\hat{t})}{s(M^2-\hat{t})} - 6\frac{(M^2-\hat{t})(M^2-\hat{u}) + M^2(\hat{t}-\hat{u})}{\hat{s}(M^2-\hat{u})}] \end{aligned} \tag{A6b}$$

$$|M|^2_{qc\to qc} = \frac{64}{9}\pi^2\alpha^2(Q^2)\frac{(M^2-\hat{u})^2 + (\hat{s}-M^2)^2 + 2M^2\hat{t}}{\hat{t}^2} \tag{A6c}$$

$$|M|^2_{gq\to gc} = \pi^2\alpha^2(Q^2)[\frac{32(\hat{s}-M^2)(M^2-\hat{u})}{\hat{t}^2} + \frac{64}{9}\frac{(\hat{s}-M^2)(M^2-\hat{u}) + 2M^2(\hat{s}+M^2)}{(\hat{s}-M^2)^2} \tag{A6d}$$

$$+\frac{64}{9}\frac{(\hat{s}-M^2)(M^2-\hat{u})+2M^2(M^2+\hat{u})}{(M^2-\hat{u})^2}+\frac{16}{9}\frac{M^2(4M^2-\hat{t})}{(\hat{s}-M^2)(M^2-\hat{u})}$$
$$+16\frac{(\hat{s}-M^2)(M^2-\hat{u})+M^2(\hat{s}-\hat{u})}{\hat{t}(\hat{s}-M^2)}-16\frac{(\hat{s}-M^2)(M^2-\hat{u})+M^2(\hat{s}-\hat{u})}{\hat{t}(M^2-\hat{u})}]$$

For the subprocesses $gg \to C\bar{C}$ and $q\bar{q} \to C\bar{C}$, we assume the following forms for the parton momenta a,b and c.

$$p_a = (\frac{x_a\sqrt{s}}{2}, 0, 0, \frac{x_a\sqrt{s}}{s}) \tag{A7a}$$
$$p_b = (\frac{x_b\sqrt{s}}{2}, 0, 0, \frac{x_b\sqrt{s}}{s}) \tag{A7b}$$
$$p_c = (M_T chy, p_T, 0, M_T shy), M_T = \sqrt{M^2+p_T^2} \tag{A7c}$$

Mandelstam variables $\hat{s} = (p_a+p_b)^2$, $\hat{t} = (p_a-p_c)^2$ and $\hat{u} = (p_b-p_c)^2$, for these subprocesses can be calculated as,

$$\hat{s} = x_a x_b S \tag{A8a}$$
$$\hat{t} = M^2 - x_a\sqrt{s}M_T exp(-y) \tag{A8b}$$
$$\hat{u} = M^2 - x_b\sqrt{s}M_T exp(y) \tag{A8c}$$

For the subprocesses involving heavy quark excitations, we assume the following forms for p_a,p_b and p_c

$$p_a = (\frac{x_a\sqrt{s}}{2}, 0, 0, \frac{x_a\sqrt{s}}{s}) \tag{A9a}$$
$$p_b = (\sqrt{M^2+\frac{x_b^2 s}{2}}, 0, 0, -\frac{x_b\sqrt{s}}{2}) \tag{A9b}$$
$$p_c = (M_T chy, p_T, 0, M_T shy) \tag{A9c}$$

Corresponding Mandelstam variables are

$$\hat{s} = M^2 + x_a x_b s \tag{A10a}$$
$$\hat{t} = M^2 - x_a\sqrt{s}M_T exp(-y) \tag{A10b}$$
$$\hat{u} = 2M^2 - x_b\sqrt{s}M_T exp(y) \tag{A10c}$$

One of the integration in Eq.A1 can be eliminated with the condition $\hat{s}+\hat{t}+\hat{u} = 2M^2$, and charm production cross section can be obtained as,

$$\frac{d\sigma^C}{dyd^2p_T} = \sum_{i,j}^{partons}\int_{x_a^{min}}^1 dx_a f_i(x_a,Q^2)f_j(x_b,Q^2)\frac{2}{\pi}\frac{x_a x_b + M_q^2/s}{2x_a - x_T exp(y)}\frac{d\sigma}{d\hat{t}}(ab\to cd) \tag{A11}$$

where

$$x_b = \frac{x_a x_T e^{-y} - 4M_q^2/s}{2x_a - x_T e^{-y}} \tag{A12}$$
$$x_a^{min} = \frac{x_T e^{y} - 4M_q^2/s}{2 - x_T e^{-y}} \tag{A13}$$

where $M_q = 0$ for the subprocesses, $gg(q\bar{q}) \to C\bar{C}$ and $M_q = M_c$ for the subprocesses, $gC \to gC$ and $qC \to qC$.

If $D_{D/C}(z,\mu^2)$ is the fragmentation function for quark C to fragment into D meson h, transverse momentum distribution of D are obtained as,

$$\frac{d\sigma^D}{dy_h d^2q_T} = \int\frac{dz}{z^2}D_{D/C}(z,\mu^2)\frac{d\sigma^C}{dyd^2p_T} \tag{A14}$$
$$= \sum_{i,j}^{partons}\int_0^1\frac{dz}{z^2}D_{D/C}(z,\mu^2)\int_{x_a^{min}}^1 dx_a f_i(x_a,Q^2)f_j(x_b,Q^2)\frac{2}{\pi}\frac{x_a x_b + M_q^2/s}{2x_a - x_T e^{y}}\frac{d\sigma}{d\hat{t}}(ab\to cd) \tag{A15}$$

For a given hadron momentum (q_T) and rapidity (y_h), corresponding quantities (p_T, y) of the fragmenting parton are obtained from the relations,

$$\sqrt{M_h^2 + q_T^2} chy_h = z\sqrt{M^2 + p_T^2} chy \tag{A16a}$$

$$\sqrt{M_h^2 + q_T^2} shy_h = \sqrt{M^2 + p_T^2} chy \tag{A16b}$$

Semileptonic decay of heavy mesons $D \to Xe\nu$ has been studied in detail [22,23]. We will not elaborate on the procedure. Transverse momentum distribution of electrons from the decay of the D-mesons can be calculated as [22],

$$\frac{dN^e}{dp_T} = \int \frac{dN^D}{dp'_T} H(p_T, p'_T) dp'_T \tag{A17}$$

with

$$H(p_T, p'_T) = \int \frac{d(p_T.p'_T)}{2|p_T|p_T.p'_T} f(\frac{p_T.p'_T}{M_D}) \tag{A18}$$

where f is the rest frame distribution of decay electrons. We have used the following rest frame spectrum for the decay $D \to Xe\nu$ [22],

$$f(E_e) = \frac{1}{\Gamma}\frac{d\Gamma}{dE_e} = wg(E_e) \tag{A19}$$

where

$$g(E_e) = \frac{E_e^2(M_D^2 - M_X^2 - 2M_D E_e}{M_D - 2E_e} \tag{A20}$$

$$w = \frac{96}{(1 - 8m^2 + 8m^6 - m^8 - 24m^4 \ln m) M_D^6} \tag{A21}$$

$$m = M_X/M_D \tag{A22}$$

We assumed that for D-mesons decay, $M_X = M_K$=0.497 GeV.

Above formulation is given in terms of charm quarks and D mesons, They are also applicable for bottom quark and B-meson production with appropriate change of masses. For semileptonic decay of B-mesons, $B \to Xe\nu$, $M_X = M_D$.

Decay electron spectra are appropriately weighted by the branching ratios. For $D \to e$ branching ratio is 0.103 and that for decay of $B \to e$ branching ratio is 0.109 [13]. We note that $B \to D \to e$ channel also contribute to total electron spectrum, but we have ignored it, as second order contribution.

---

* e-mail:akc@veccal.ernet.in

[1] J. Adams et al [STAR Collab.], Phys. Rev. Lett. 94 (2005)062301 [arXiv:nucl-ex/0407006]; An Tai [STAR Collab.], J. Phys. G30 (2004)S809, [arXiv:nucl-ex/0404029].
[2] S. S. Alder et al [PHENIX collab.], Phys. Rev. Lett.94(2005)082301; S. Kelly [PHENIX Collab.], [arXiv:nucl-ex/0403057].
[3] J. Adams et al, STAR Collaboration, Phys.Rev.Lett.91, 2003,072304,nucl-ex/0306024. Phys.Rev.Lett.91, 2003,172302,nucl-ex/0305015. Phys.Rev.Lett.89, 2002,202301,nucl-ex/0206011.
[4] S. S. Alder et al, PHENIX collaboration, Phys.Rev.C69,2004, 034910, nucl-ex/0308006. Phys.Rev.Lett.91,2003,072303, nucl-ex/0306021. Phys.Rev.Lett.91,2003,072301, nucl-ex/0304022
[5] B. B. Back et al., PHOBOS collab. Phys.Rev.Lett.91,2003,072302, nucl-ex/0306025. Phys.Lett.B578 2004, 297.
[6] I. Arsene, BRAHMS collab., Phys.Rev.Lett.91,2003, 072305.
[7] M. Gyulassy and M. Plumer, Phys. Lett. B243, 1990, 432.
[8] X. N. Wang and M. Gyulassy, Phys.Rev. Lett. 68 (1992) 1470.
[9] T. Matsui and H. Satz, Phys. Lett. B178,416(1986).
[10] R. L. Thews, M. Schroedter and J. Rafelski, Phys. Rev. C63(2001)054905.
[11] M. Cacciari, M. Greco and Paolo Nason, [arXiv:hep-ph/9803400].

[12] R. Vogt, [arXiv;hep-ph/0203151].
[13] M. cacciari, P. Nason and R. Vogt, [arXiv:hep-ph/0502203].
[14] K. J. Eskola and H. Honkanen, Nucl. Phys. A713, 167(2003).
[15] E. Braaten, K. Cheung, S. Fleming and T. C. Yuan, Phys. Rev. D51 (1995)4819.
[16] C. Peterson, D. Schlatter, I. Schmitt and P. M. Zerwas, Phys. Rev. D27 (19982)105.
[17] V. G. Kartvelishvili, A. K. Likhoded and V.A. Petrov, Phys. Lett. B78(1978)615.
[18] P. Collins and T. Spiller, J. Phys. G11 (1985)1289.
[19] T. Sjoestrand et al, Comput. Phys. Commun. 135(2001)238.
[20] G. Sterman et al, Rev. Mod. Phys, 67 (1995)157.
[21] B. L. Combridge, Nucl. Phys. B151(1979)429.
[22] M. Gronau, C. H. Llewllyn Smith, T. F. Walsh, S. Wolfram and T. C. Yang, Nucl. Phys. B123 (1977)47.
[23] A. Ali, Z. Phys. C1(1979)23, CERN-TH-2411